

Article

The Role of Soil Stabilisation in Mitigating the Impact of Climate Change in Transport Infrastructure with Reference to Wetting Processes

Ana Heitor ^{1,*}, Joshua Parkinson ² and Thomas Kotzur ³¹ School of Civil Engineering, University of Leeds, Leeds LS2 9JT, UK² Aurecon, Sydney, Australia, Formerly School for Civil, Mining and Environmental Engineering, University of Wollongong, Wollongong, NSW 2522, Australia; Joshua.Parkinson@aurecongroup.com³ Thiess, Mount Pleasant, Australia, Formerly School for Civil, Mining and Environmental Engineering, University of Wollongong, Wollongong, NSW 2522, Australia; tkotzur@thiess.com.au

* Correspondence: a.heitor@leeds.ac.uk; Tel.: +44-7849282475

Abstract: Cost efficient and robust transport systems are of critical importance to future economic prosperity as well as for the society's social and environmental well-being. However, current performance shortcomings in the transport infrastructure formations induced by extreme climatic events cause excessive maintenance requirements with increased costs and disruptions to commuters and loss of productivity in the freight services. This is particularly important in locations where soils are sensitive to moisture changes caused by extreme climatic events. In this paper the role of soil stabilisation in halting volumetric deformation and associated reduction in shear strength derived from the wetting processes (e.g., rainfall periods) is examined for an expansive soil. Two stabilizers commonly used in road construction are examined, i.e., hydrated lime and Portland cement. An additional non-traditional stabiliser composed of a blend of ground granulated blast furnace slag and hydrated lime is also considered. A series of one-dimensional swelling and direct shear box tests were conducted adopting vertical stresses relevant for pavements and simulate wetting process that can take place after a period of rainfall. Results indicate that while all stabilizers contribute to a reduction of swelling and smaller losses in shear strength upon wetting, the blend of blast furnace slag and hydrated lime is the most favourable in terms of carbon footprint.

Keywords: climate change; expansive soil; soil stabilisation; pavements



Citation: Heitor, A.; Parkinson, J.; Kotzur, T. The Role of Soil Stabilisation in Mitigating the Impact of Climate Change in Transport Infrastructure with Reference to Wetting Processes. *Appl. Sci.* **2021**, *11*, 1080. <https://doi.org/10.3390/app11031080>

Received: 1 December 2020

Accepted: 18 January 2021

Published: 25 January 2021

Publisher's Note: MDPI stays neutral with regard to jurisdictional claims in published maps and institutional affiliations.



Copyright: © 2021 by the authors. Licensee MDPI, Basel, Switzerland. This article is an open access article distributed under the terms and conditions of the Creative Commons Attribution (CC BY) license (<https://creativecommons.org/licenses/by/4.0/>).

1. Introduction

Current performance shortcomings in the transport infrastructure formations induced by extreme climatic events cause excessive maintenance requirements with increased costs and disruptions to commuters and loss of productivity in the freight services. Most transport infrastructure formations are essentially compacted, hence remain unsaturated under capillarity stresses or matric suction [1], which influences their hydro-geomechanical response, e.g., water retention behaviour and unsaturated permeability [2], microstructure and stress-strain behaviour [3]. Their post-compaction behaviour in cycles of wetting and drying caused by rainfall and drought periods, respectively, is also strongly influenced by the initial compacted state [4]. Past studies showed that the behaviour of compacted soil is governed by the initial compacted state ([5–7]). This is particularly important in the areas where local conditions can be unfavourable due to the existence of expansive soils. In these locations, the assessment of the in-service performance of the subgrade soils under notable variations in subsurface moisture caused by climate change; i.e., intense periods of rainfall and droughts (e.g., wetting and drying) becomes critical in design. For instance, [8] reported that the volumetric changes associated with shrink and swell processes in expansive soil subgrades upon seasonal wetting and drying causes the onset

of cracking in pavements, which is then further exacerbated as moisture ingress increases. The rising cost of pavement rehabilitation continues to drive engineers to investigate more economically solutions to improve the performance of high plasticity clays when exposed to seasonal changes in moisture.

In this paper, the role of soil stabilisation in halting volumetric deformation of expansive soils is examined and associated reduction in shear strength derived from the wetting processes (e.g., rainfall periods).

1.1. Climate Change in Australia

The consideration of the effects of climate change in Australia have become critical in last decade, as many locations are now prone to extreme heat, bushfires, droughts, floods and longer fire seasons ([9]). Figure 1 shows the mean temperature and annual rainfall deciles for Australian states and territories for the period of 1 February 2019 to 31 January 2020.

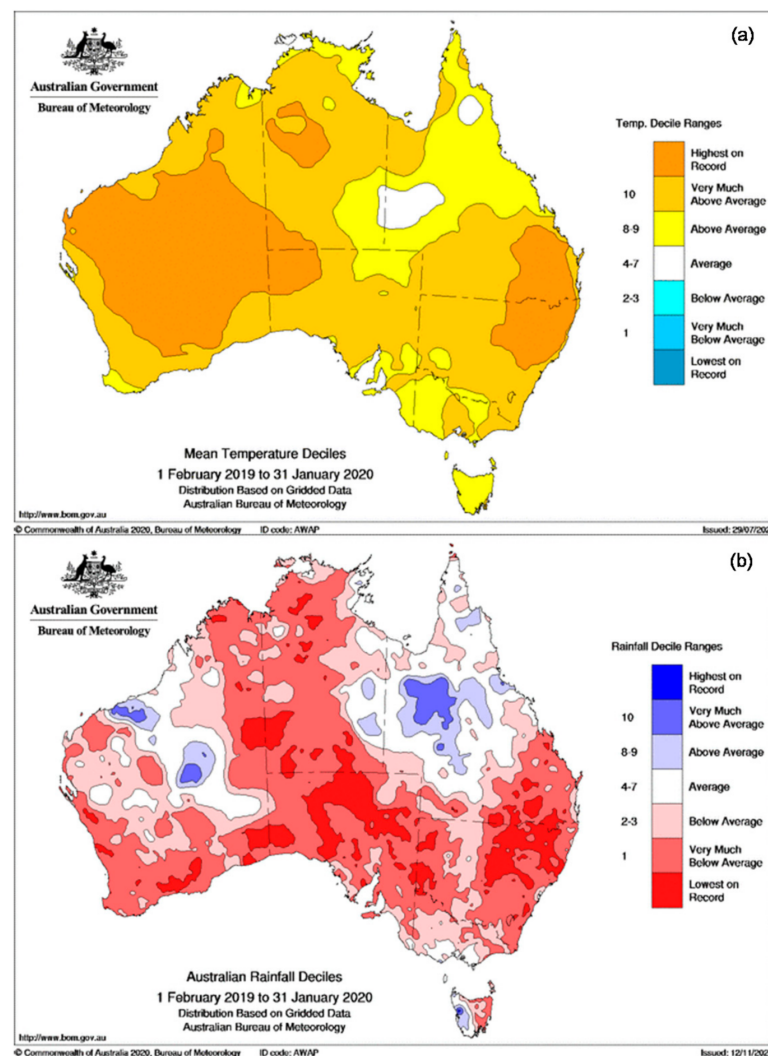


Figure 1. Climate change effect on (a) mean temperature and (b) rainfall in Australia based on all years of data since 1910 ([10], reproduced under the Creative Commons Attribution Australia Licence <https://creativecommons.org/licenses/by/3.0/au/legalcode>).

It should be noted that the average temperature and rainfall benchmarks are based on data collected from 1910. It can be observed that for the 12-month period shown in Figure 1, a great percentage of their territories recorded the highest on record mean temperature with greater prevalence in the Western Australia state. Except for the state of Queensland

and areas of Western Australia and Tasmania which recorded the highest on record annual rainfall, most Australian states and territories recorded annual rainfall below average or lowest on record. This deciles maps trends illustrate the incidence of extremely high temperatures and widespread drought in Australia and that rainfall is expected to become heavier and more infrequent. These extreme climatic changes year upon year can have a dramatic influence on the performance of built infrastructure particularly transport assets (road and rail) located where there is a greater incidence of soils with high susceptibility for volume change upon a variation in moisture.

1.2. Expansive Soils

An estimated 2.4 million km² of the expansive soil can be found worldwide, with Australia accounting for approximately 800,000 km² of this total [11]. These soils are located discontinuously across Australia (Figure 2) and are notorious for causing extensive damage to infrastructure in locations prone to extreme weather events including droughts and floods.

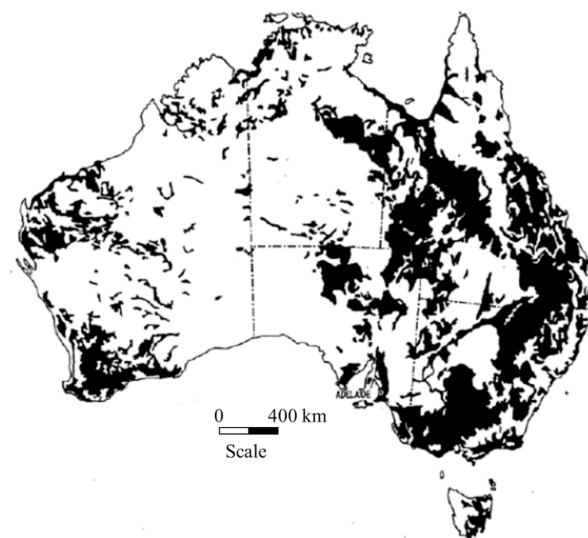


Figure 2. Distribution of moderately to highly expansive soils in Australia (after [12]).

During periods of drought, the moisture is lost in the clay causing the ground to shrink. This results in shrinkage occurring in the subgrade often resulting in large cracks forming and propagating through the pavement. In contrast, during large rainfall events often resulting in flooding, the material experiences wetting, resulting in swelling and substantial loss in the shear strength. The use of chemical additives can improve the subgrade conditions during these extreme climatic events. While past research has extensively developed analytical models to estimate the magnitude of swell of these soils from basic properties ([13–18]) limited research studies have focussed on the role of soil stabilisation in controlling swelling and the reduction in shear strength as a result of wetting.

The swelling properties of clays are highly dependent on their mineral composition. Swelling occurs when water molecules surrounding a clay particle, position themselves to increase the c-spacing between clay mineral layers. This causes an increase in the volume of the clay, causing the clay to expand. This swelling can occur from two mechanisms [19], hydration swelling and osmotic swelling. Hydration swelling occurs when hydrogen bonds form between water molecules and oxygen atoms on the surface of the clay minerals. As subsequent layers add to these bonds, the water molecules form a lattice within the clay. This expands the basal spacing between atoms, thus causing swelling of the clay. In contrast, osmotic swelling occurs due to the build-up of cations on the surface of the clay. If the concentration of exchangeable cations on the clay surface exceeds the concentration in the water, the water will attract to the clay surface to balance this. This leads to a build-up

of water between layers in the soil, causing an increase in the c-spacing between mineral layers, resulting in swelling. While the role of osmotic swelling is important, it is the hydration swelling process that induces greater volumetric changes during wetting and drying process that the soil is likely to experience as result of climatic events.

2. Materials and Testing Program

2.1. Soil

The soil selected for this study was procured through Road and Maritime Services in conjunction with the Newell Highway Corridor Strategy (NHCS). The samples were taken from the road widening activities and road rehabilitation project located at North Gurley (south of Moree). The main soil properties are given in Table 1. It can be classified as a very high plasticity clay or CV (Unified Soil Classification System). The particle size distribution of the soil is shown in Figure 3 and represents 2% gravel, 35% sand, 60% silt and 2% clay. The fine fraction of the particle size distribution was obtained using laser diffraction technique (Malvern mastersizer 3000), which represents the distribution of particles in relation to particle diameter vs. percentage of total particle volume. A technique considering the specific gravity and particles as spheres was adopted to convert from a volume to a mass-based PSD, which introduced some inaccuracies, associated with the approximation of particle shape adopted. While the clay content shown in Figure 3 may be considered unusually small for a soil exhibiting moisture sensitiveness according to well-established expansive soil classifications [20], ref. [21] report that the hydrometer method systematically overestimates the clay fraction respect to the laser diffraction method. Hence, the soil used on this study was classified mainly from a behavioural standpoint. The activity of the soil calculated based on the ratio of the plasticity index and mass percentage of particles smaller than 0.002 mm, was found to be 25.4 which can be classified as very high activity (>1.25) and indicates the soil tested is expansive. Furthermore, the weight plasticity index is 4300 which indicates that this soil has a very high potential for volume change [22]. A summary of the soil index properties is given in Table 1.

Table 1. Summary of the soil properties tested.

Property	Value
Liquid limit (LL)	73%
Plastic Limit (PL)	31%
Plasticity Index (PI)	42%
Mass percentage of particles smaller than 0.002 mm	2%
Weighted PI = PI \times % passing 425 μ m	4300
Optimum moisture content (OMC)	27%
Maximum dry unit weight (MDUW)	14.9 kN/m ³

The soil samples were first dried (105 °C for 24 h) and then the clusters of clay were disaggregated using a mechanical crusher. The soil was then sieved and any particles greater than 2 mm were removed, as to reduce the impact of oversize particles on the swell and shearing of soil specimens, as specified in ASTM D4546. Deionised water and required amount of chemical admixture was added and thoroughly mixed to bring the soil to the required moisture content determined based on its compaction characteristics.

The soil specimens having the specified water content and chemical admixture were compacted in oedometer rings and shear box mould to the required dry unit weight to meet compaction requirements, e.g., 95% maximum dry unit weight ($\gamma_d = 14.1 \text{ kN/m}^3$) and 75% of moisture content ($w = 20\%$). However, for the soil specimens used in the swelling tests, a relative compaction of 100% was chosen instead of the minimum of 95%. This is due to the increased swelling experienced at higher compaction levels [23], meaning the critical swelling state will be at a higher level of compaction.

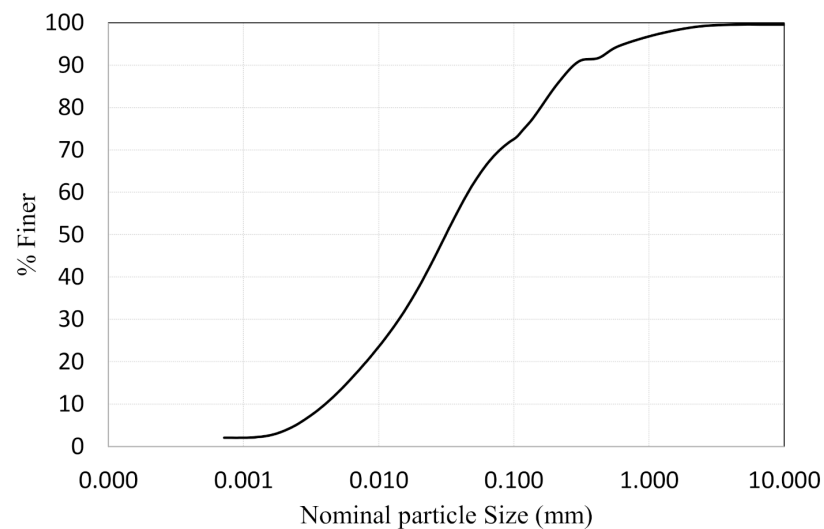


Figure 3. Particle size distribution.

These values were selected to mimic subgrade conditions observed in the field when constructing roads in New South Wales (Australia). The mass of each specimen was recorded, before the samples were sealed with a thin plastic film and kept for 24 h in constant temperature and humidity conditions for allowing moisture equilibration. Additional material was also prepared for checking moisture content of the soil for verification.

2.2. Hydraulic Binders

The hydraulic binders adopted in this study are recommended for fine grained soils having plasticity index (PI) larger 20 by [24] and are used widely in road construction, i.e., hydrated lime (HL), Portland cement (PC). While there are other methods of chemical stabilization commonly adopted in construction projects such as: quick lime, pozzolana, lime-pozzolana mixtures, polymers, resins, fly ash or bituminous material, in this study hydrated lime, Portland cement were adopted. This is in line with the recommendations provided with Austroads (collective of the Australian and New Zealand transport agencies, representing all levels of government) for a soil having a plasticity index (PI) larger than 20. An additional stabiliser composed of a blend of ground granulated blast furnace slag and hydrated lime (BFS/HL) mixed in 70/30 dry weight proportion was considered to evaluate the performance of a non-traditional stabiliser. Ground granulated blast furnace slag is a granular waste by-product of the iron and steel industry produced by quenching the molten slag. While a proportion of slag is still landfilled currently, in the recent decade there have been important research efforts to support their use in the concrete industry and as fill material [25], although applications in soil stabilisation have been limited. This is likely because while ground granulated blast furnace slag has a high calcium oxide content, it needs an alkali activator to kick start the hydration (pozzolanic) reaction. In this study a small amount of hydrated lime was used. The chemical composition of the different stabilisers is shown in Table 2. The stabilizers were added to the soil in different percentages calculated on a dry weight basis prior compaction. The stabilizer percentages adopted were based on common levels of treatment implemented for expansive soil, e.g., percentages smaller than 4%.

Table 2. Chemical composition of hydrated lime and Portland cement (data from [26]) and blast furnace slag chemical composition (data from [27]).

Hydrated Lime	
Chemical Entity	Proportion
H ₂ O	0.1–2.5%
Ca(OH) ₂	90–95%
Mg(OH) ₂	0.5–1%
SiO ₂	0.5–3%
Al ₂ O ₃	0–2%
FeO	0–0.4%
Portland Cement	
Portland Clinker	<97%
CaSO ₄ 2H ₂ O	2–5%
CaCO ₃	0–7.5%
CaO	0–1%
Cr (VI)	<10 ppm
Blast Furnace Slag:	
Constituent	
CaO	35–42%
SiO ₂	33–38%
Al ₂ O ₃	10–15%
MgO	7–12%
FeO	<1%
MnO	<1%
Cr ₂ O ₃	<0.1%

2.3. Swelling Tests

The testing procedure was conducted in accordance with Test Method A outlined in ASTM D4546. Dry filter paper was applied to the top and bottom of each sample, as stated in ASTM D4546. The samples were then loaded incrementally, with each additional increment load given 10 min to allow settlement to occur before additional load was added.

The samples were then inundated, and measurements of the swell were taken at time intervals of 0.5 min, 1 min, 2 min, 4 min, 8 min, 15 min, 30 min, 1 h, 2 h, 4 h, 8 h and 24 h. Before the test was complete, the water was removed from the oedometer apparatus, and the samples were removed and weighed. The specimens were then oven-dried, and their final moisture content could be determined.

The pH of the water at the end of the tested was also evaluated to assess whether the use of these stabilisers could cause detrimental impacts to environment due to alkaline leaching. The pH showed an increase from 7 for unstabilised specimens to 11–12 for the treated specimens.

2.4. Direct Shear Box Tests

The direct shear testing was carried out in accordance with Australian standard AS 1289.6.2.2-1998. The vertical stress applied to the specimen during shearing in the direct shear box was 35 kPa because this is equivalent to the self-weight of the pavement above the subgrade. A shear rate of 0.5 mm/min was adopted, and the shear stress and vertical displacement were monitored during shearing. To examine the influence of wetting, selected specimens were inundated for 24 h to mimic infiltration processes that would take place after rainfall periods and shearing resumed subsequently. The specimens were inundated at three stages of shearing (a) prior to shearing to evaluate as compacted conditions, i.e., new build, (b) once the soil reached yield mimicking most of the stress states the soil is likely to experience during the service life of the infrastructure. The shear tests aim to investigate the stress-strain behaviour of the soil at the subgrade level near the pavement shoulders (i.e., vertical stress of 35 kPa) and assess whether any potential

localised failures could arise from the wetting process and loss of strength. The direct shear apparatus was preferred because of its ease in inundating specimens compared to triaxial testing.

2.5. Microstructural Imaging

The structure of stabilised soil was probed using a scanning electron microscope (SEM) model JEOL JSM-6490LA housed at the microscopy facility of the University of Wollongong. A scanning electron microscope (SEM) capable of testing both in high and low vacuum settings was used in this study. This type of SEM can also be referred to as ESEM and can operate at low vacuum, which allows the testing of specimens in a moist condition, thus avoiding undesirable microstructural damage that can result from the drying process. The soil specimens were imaged at different magnifications to examine the microstructural effects of each stabiliser on various scales. Soil specimens were imaged before and after inundation. For each specimen, an Energy Dispersive X-ray Spectroscopy (EDS) test was also conducted. The EDS graphs show the distribution of different elements in the soil, which can indicate the presence and increase in the elements associated with the stabilisers (e.g., calcium, carbon, sulphur and heavy metals). Figure 4 shows the Energy Dispersive X-ray Spectroscopy (EDS) spectrum for the soil studied having no treatment.

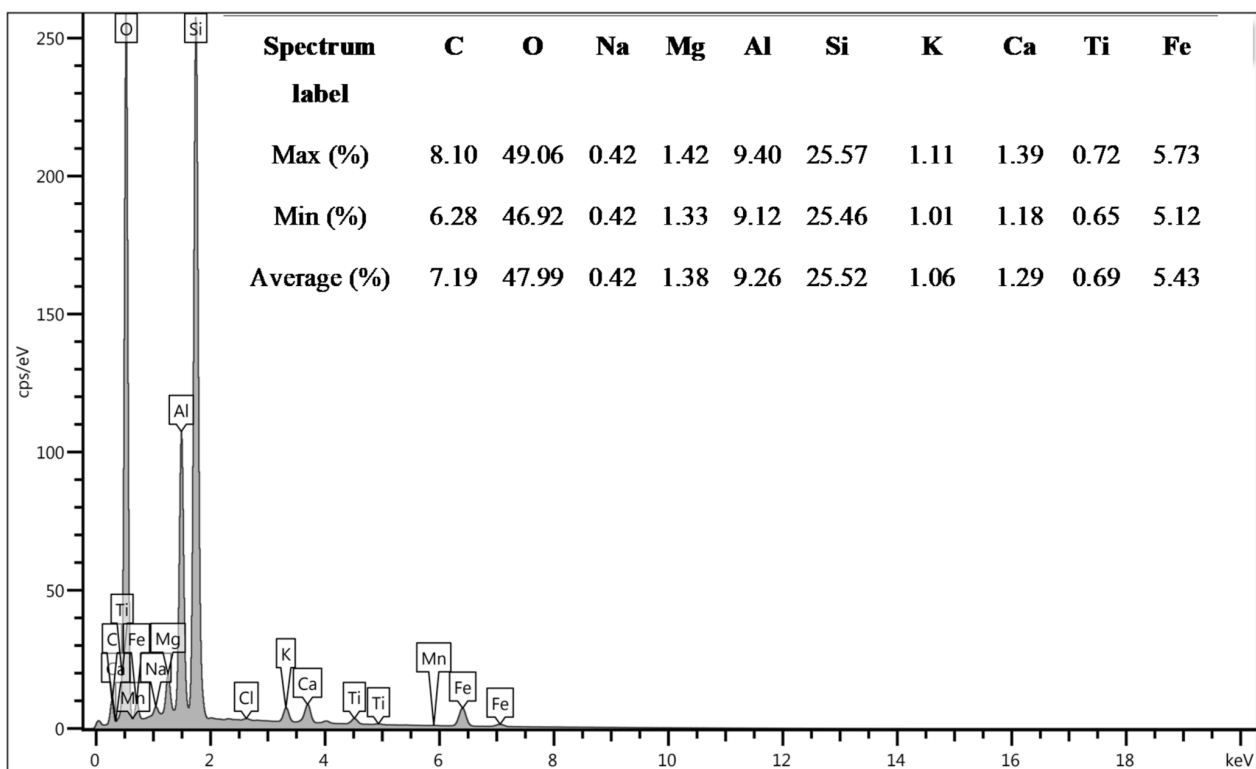
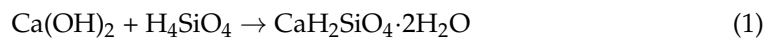


Figure 4. EDS spectrum of the unstabilised soil.

3. Results and Discussion

The results of the Atterberg limits tests conducted in the soil samples having different percentages of the stabiliser addition are shown in Figure 5a. As expected, the addition of the stabilizers has substantial influence on the plasticity of the soil contributing to a reduction in the liquid limit and an increase in the plastic limit, albeit smaller for the latter. From the three stabilisers, the addition of hydrated lime induces the greatest reduction in liquid limit whereas Portland cement influences the increase in plastic limit to a greater extent. This is illustrated in Figure 5b where the variation in relation to the values obtained for the non-stabilised soil is shown, i.e., positive and negative variation indicates an increase

and decrease in the values, respectively. While both hydrated lime and Portland cement have comparable reduction in plasticity index (PI) the mechanism causing those changes is different. This is likely associated to changes in soil chemistry taking place when the stabilizer is added, i.e., while the onset of pozzolanic reactions (Equation (1)) is present for both stabilisers, the silicon source required to catalyse the reaction is different. In lime stabilization, the silicon mainly results from the breakdown of the clay minerals as hydrated lime has negligible silica content (Table 2). In contrast, in cement stabilization, silicon is available in the form of silicon dioxide (SiO₂) approximately in the same proportion as calcium oxide (CaO) (Table 2). This also corroborated by the larger reduction of silicon levels observed through EDS testing of the samples treated with the hydrated lime.



The experimental trends reported herein are in line with experimental observations reported for other high plasticity soils in past studies focusing on the effect of lime and cement stabilization (e.g., [28]) on the Atterberg limits.

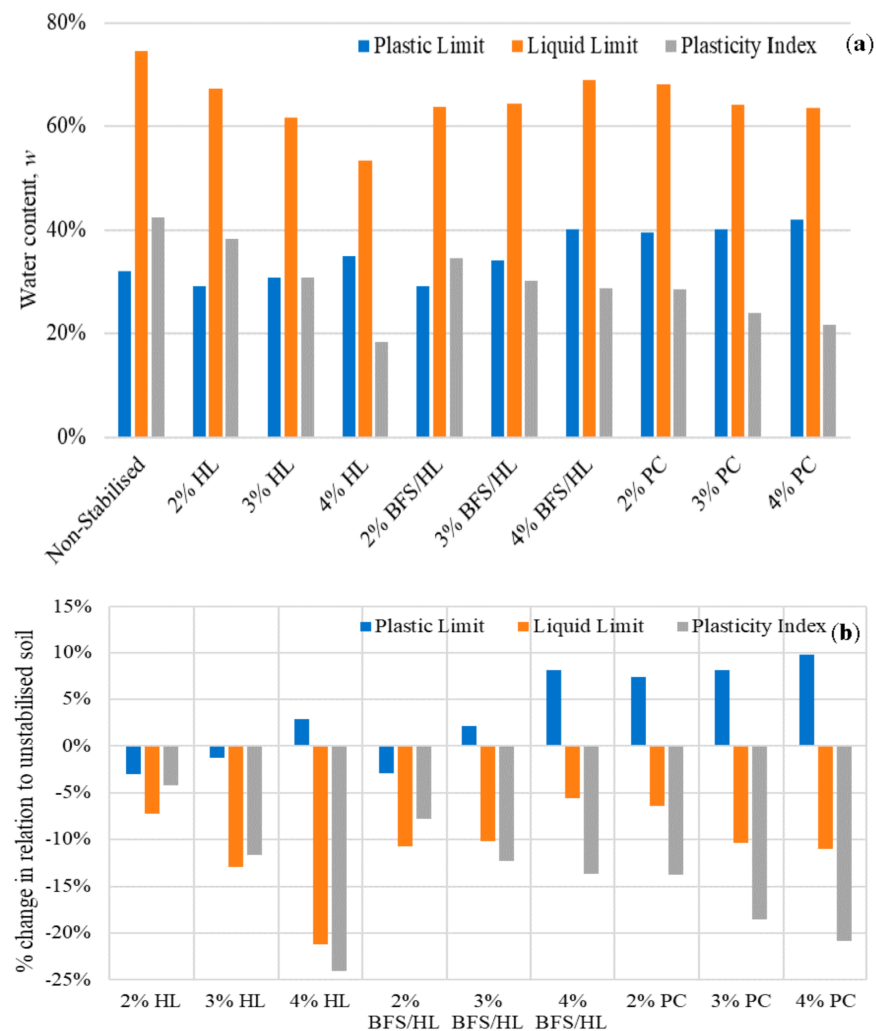


Figure 5. Summary of the results of soil index testing (Atterberg limits) having different levels of added chemical stabilisers (a) test results and (b) percentage variation of water content in relation to the non-stabilised soil (HL—Hydrated lime, BFS/HL—70/30 blend of ground granulated blast furnace slag and hydrated lime and PC-Portland cement).

A series of one-dimensional swelling tests were conducted for selected treatment levels of 2% and 4% by weight. The efficiency of the treatment was evaluated for different vertical

stress levels in term of its influence in halting swelling, i.e., positive volumetric change. Figure 6 shows a summary of the results obtained. As expected upon inundation the non-stabilised specimen exhibit mainly swelling behaviour except for the largest vertical stress level adopted (i.e., 50 kPa) where compression (consolidation) dominated the soil behaviour. The role of the stabilizer addition in halting swelling (0–25 kPa vertical stress) or reducing compression (50 kPa vertical stress) are better illustrated in Figure 6b. It can be observed that all stabilisers considered, i.e., Portland cement, hydrated lime and a blend of ground granulated blast furnace slag and hydrated lime are effective in reducing swelling and compression. However, the one showing greatest performance for the same level of treatment is hydrated lime at 4% addition on a dry weight basis. Furthermore, while at 4% addition, Portland cement is the least effective pozzolanic stabiliser tested for reducing swelling is the best performer in terms of reducing compression. This could indicate that the chemical processes taking place between the cement and clay are ineffective at reducing the uptake of water into the interlayer space of the silicate clay basal spacing but the pozzolanic reaction products induce some cementation at the particle’s contacts that contribute to a reduction of compression behaviour, also observed in the SEM micrographs (Figure 6). Interestingly, the blend of ground granulated blast furnace slag and hydrated lime stabiliser has comparable performance to hydrated lime in reducing swelling but is slightly less effective in reducing compression (Figure 6b).

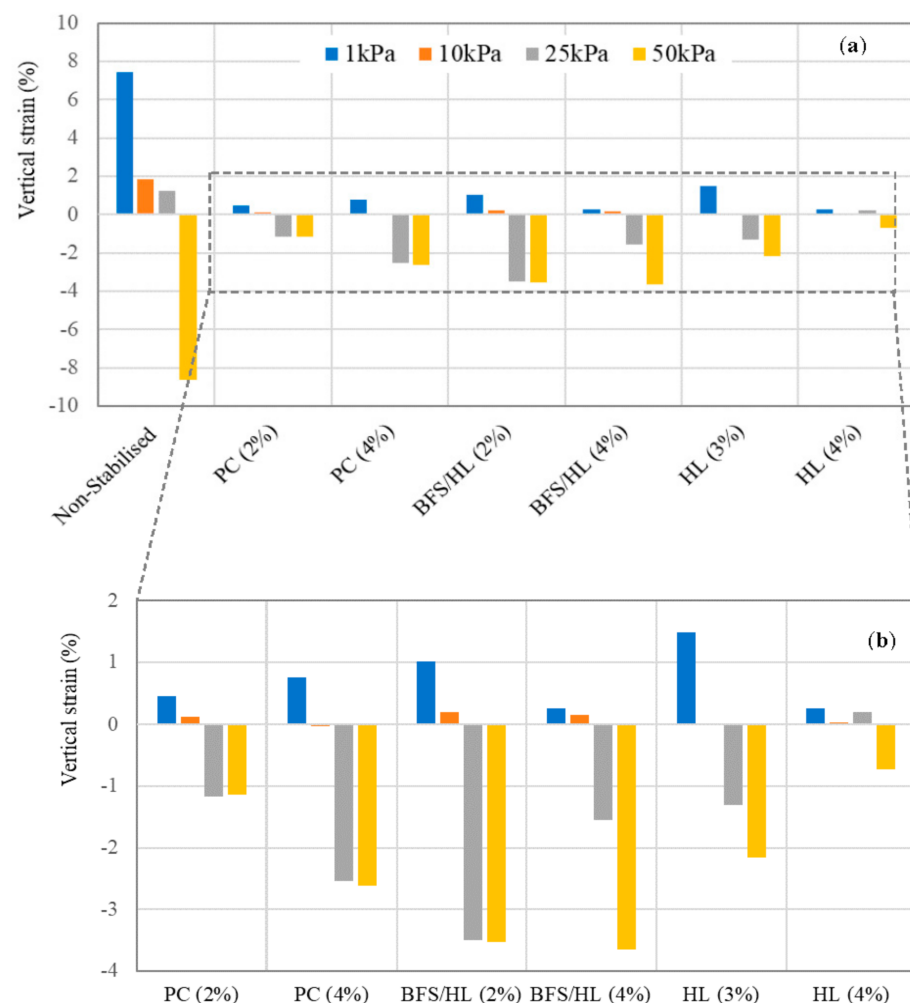


Figure 6. Summary of the (a) vertical strains obtained in the swelling tests under various vertical stresses, i.e., positive values indicate swelling whereas negative values indicate consolidation and (b) magnification of the results for specimens stabilised.

A series of shear box tests were conducted on specimens stabilised with 3% on a dry weight basis of additive. To evaluate the role of the stabiliser in the shear strength behaviour two different test conditions were investigated, i.e., shear behaviour representative of the as-compacted condition and post yield behaviour after inundation. The latter condition was adopted to simulate the loss of strength potentially incurred as a result of a rainfall event leading to water infiltration in a road pavement underlain by expansive soils. As expected, in the specimens tested in as-compacted condition (Figure 7a,c) the addition of the stabiliser has a substantial effect on the stress-strain behaviour. While all specimens mainly showed a strain softening and dilation response, this behaviour is more pronounced in the specimens treated with HL, PC and BFS/HL. Moreover, the specimens treated with HL and BFS/HL achieved comparable peak stresses (80–82 kPa), while those prepared with PC showed slightly lower peak stress (71 kPa). Interestingly, while there was a substantial increase in peak stress compared to the unstabilised specimen, this was not observed for ultimate states. In fact, with exception of the specimen treated with PC (50 kPa), all other specimens approached ultimate state at approximately the same stress level (42–45 kPa). This seems to indicate that when the ultimate state is reached, the shear strength of these specimens is relatively independent of the level of treatment. This is likely due to a process of destructuralization of the soil microstructure taking place during shearing. The results of the shear behaviour of the specimens inundated at yield (i.e., specimen allowed to reach yield stress before saturation) is shown in Figure 7b,d. It can be observed that for all specimens, the soil still retains its ultimate shear strength (saturated) in the secondary shearing phase. Similarly, to as-compacted condition, the unstabilised specimen achieved the lowest shear strength at ultimate state (19 kPa), with the specimen stabilised with PC showing the highest ultimate stress (34 kPa). Additionally worthy of note is the fact that all the specimens stabilised still retained shear strength during inundation, with the specimen treated with PC showing the smallest decrease in shear stress. While this may not seem the most intuitive behaviour at first sight, it may be explained from a microstructural standpoint. As a result of the pozzolanic reactions taking place during hydration (as-compacted water content), the cementation products bind the soil particles resulting in a residual shear strength upon inundation. The cementation products are more evident in the specimens treated with PC as verified by SEM micrographs (Figure 8), hence the smaller reduction in shear strength despite showing comparable ultimate shear stresses, i.e., 24 kPa, 28 kPa and 34 kPa for HL, BFS/HL and PC, respectively. In addition, in post inundation only the specimen treated with PC showed a predominantly strain softening behaviour. The untreated specimen also experienced the greatest degree of swelling upon inundation (e.g., 4.4% of the specimen original height) while the treated specimens showed much smaller level of swelling upon inundation, although the specimen treated with BFS/HL showed the largest swell (0.34 mm). Furthermore, during the secondary shearing only the specimen treated with PC exhibit mainly dilative response, while those prepared with HL and BFS/HL showed mild compression, in line with the stress-strain response observed.

The SEM micrographs illustrate the structural effects of each stabiliser on the soil microstructure and the impacts of the chemical reactions which have taken place in each specimen. Figure 8 shows selected micrographs that illustrate the noticeably rougher soil microstructure in the specimens prepared with the pozzolanic stabilisers, along with the presence of heavier elements (denoted by light specs on the images, also indicated by arrows). Interestingly the soil microstructure of specimens prepared with HL and BFS/HL is similar, indicating that hydrated lime proportion in the blend may dominate the stabilisation mechanism. Furthermore, the micrographs of specimens treated with cement show the formation of large crystals of hydrous calcium aluminium sulphate or ettringite. While the HL and BSF/HL also show the presence of these type of crystals, they are much smaller by comparison. For each sample, an Energy Dispersive X-ray Spectroscopy (EDS) was also conducted. The EDS spectrum show the distribution of different elements in the soil (Table 3), which can indicate the presence and increase in the elements associated with

the stabilisers (calcium, carbon, sulphur and heavy metals). As expected, the soil tested showed high quantities of basic clay elements (aluminium, silicon, oxygen).

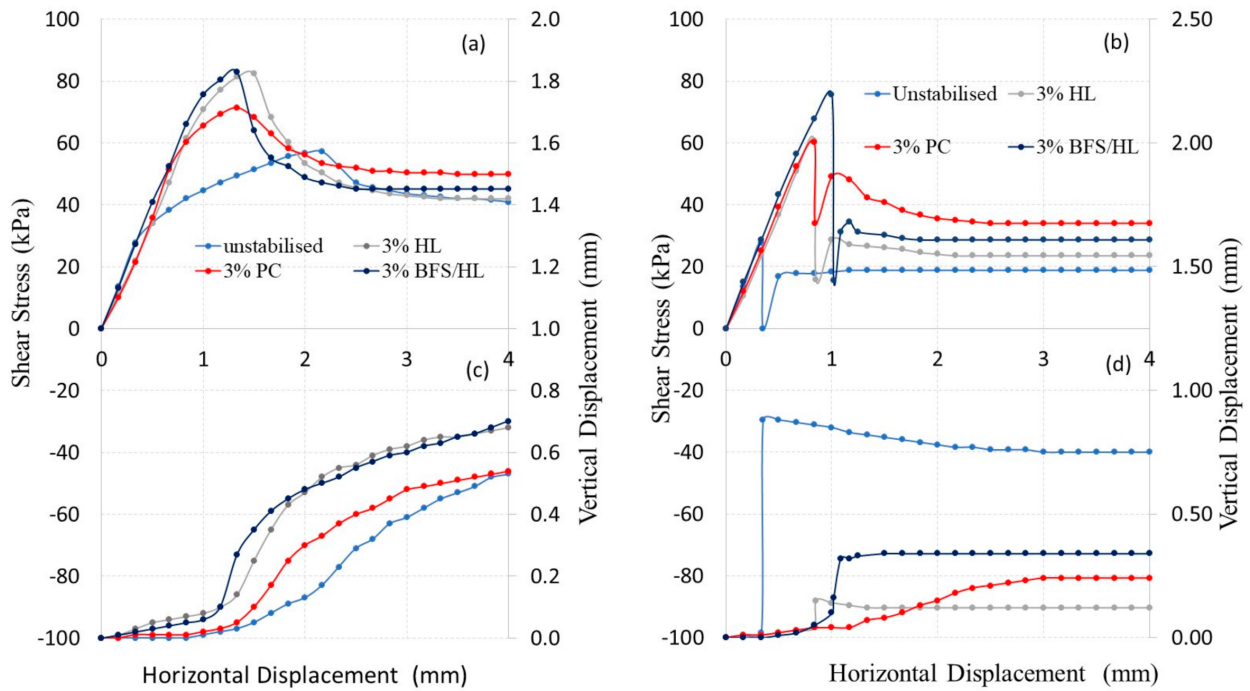


Figure 7. Summary of the shear box tests (a,c) as-compacted condition and (b,d) inundation at yield.

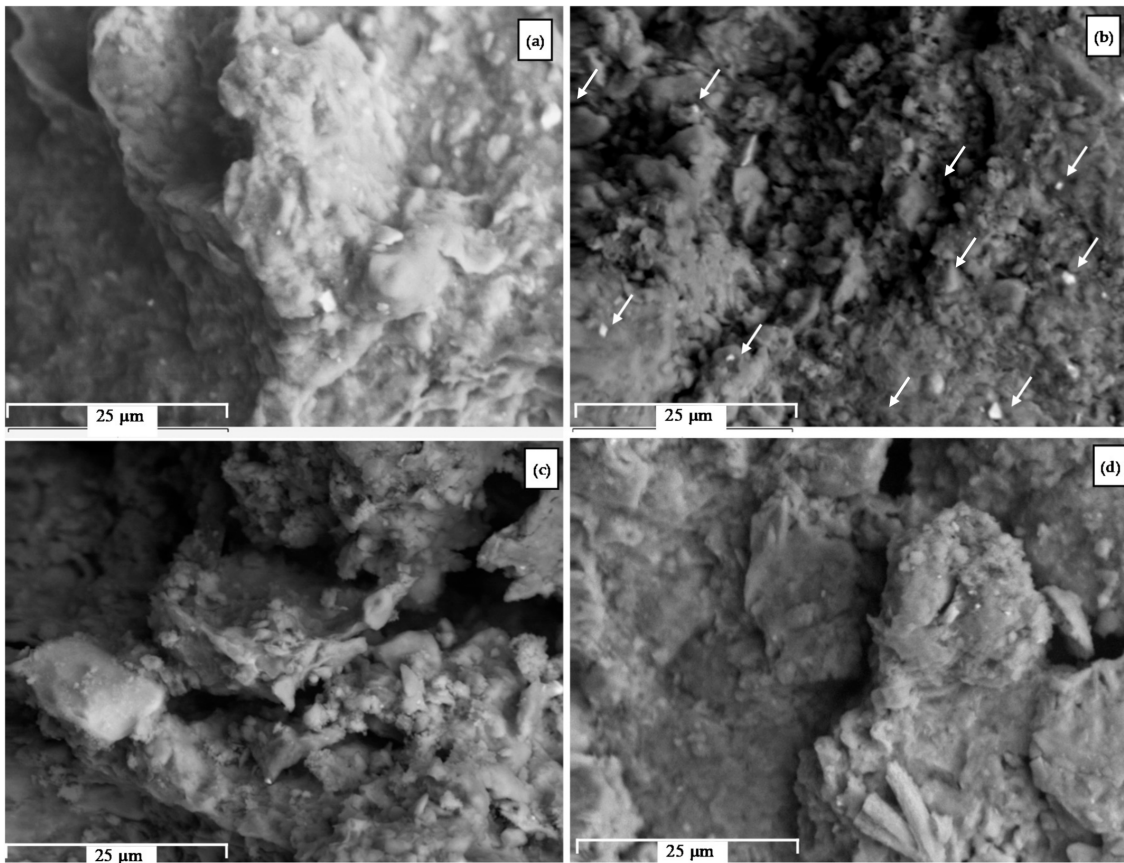


Figure 8. Summary of SEM micrographs of soil stabilised with (a) 0% stabiliser, (b) 4% HL, (c) 4% BFS/HL and (d) 4% Portland cement.

Table 3. EDS spectrum results presented as an average percentage.

Spectrum Element Label	C	O	Na	Mg	Al	Si	K	Ca	Ti	Fe
Unstabilised Average (%)	7.19	47.99	0.42	1.38	9.26	25.52	1.06	1.29	0.69	5.43
HL Average (%)	14.12	47.36	0.1	1.21	5.45	14.72	0.56	12.51	0.85	3.65
HL/SFS Average (%)	7.26	45.92	0.23	1.40	6.09	20.32	0.57	4.94	0.54	7.95
PC Average (%)	15.09	44.89	0.47	0.66	8.60	15.57	1.24	14.79	0.45	3.62

All specimens treated showed substantial increase in the calcium content, along with smaller noticeable changes in the levels of carbon, iron and aluminium. The increase in iron (Fe) in the BSF/HL blends is not surprising as ground granulated blast furnace is a waste product derived from the steel making industry and the prevalence of these element in the material is likely to be high, albeit in small amounts (Table 2).

4. Impact of Climate Change and Practical Implications

The stability of an embankment supporting a roadway is strongly related the increase in water content or reduction of matric suction in the subgrade soil and embankment fill materials. The magnitude of the changes in moisture content are in turn related to the weather conditions (e.g., rainfall, temperature, humidity, infiltration/evaporation potential), and their impact is directly associated with the soil properties (e.g., plasticity, water retention and thermal properties).

The impact climate change is twofold, i.e., (a) increase in temperature and extensive periods of droughts and (b) different rainfall patterns, which are expected to become few and far between but having a high intensity leading to rapid flooding. In other words, dry summer periods remove water that leads to shrinkage and cracking; prolonged and intense rainfall events cause swelling and increased pore water pressures. Figure 9 illustrates the effects of seasonal climatic variation on a typical roadway embankment. As it can be observed, the increase in temperature caused by atmospheric conditions will cause evaporation to take place and hence a reduction in water content (dry season). This may cause a change in the soil properties as well as the onset of cracking caused by desiccation and soil shrinkage which can propagate through the pavement layers. This is particularly important in locations with soils that have potential for volume changes (e.g., swelling and shrinkage), especially because repeated shrink-swell cycles can lead to accumulation of shear strains resulting in strain softening and progressive failure [29].

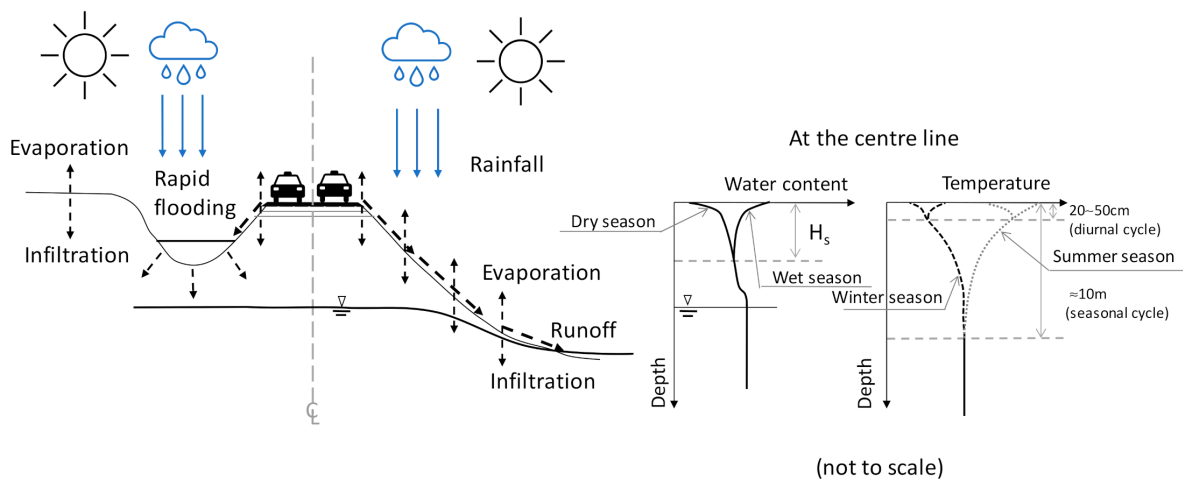


Figure 9. Diagram of a roadway embankment subjected to seasonal climatic variations.

For constant suction conditions [30] reported that the contribution of suction to soil strength and stiffness may be reduced due to thermal loading. In addition, [31] reported that an increase in temperature from 20 to 60 °C under approximately the same level of suction results in a reduction in the soil shear strength and resilient modulus due to the differences in surface tension values at these temperatures. Nonetheless, it should be noted that temperature changes induced by climatic action as illustrated in Figure 9 are likely to be accompanied by a variation of moisture and suction. The soil thermal regime can be characterized by periodic changes in response to the natural periodicity in atmospheric conditions. There is a diurnal (daily) cycle, as well as a superimposed seasonal cycle (Figure 9). In the diurnal cycle, the temperature variation in the soil tends to be shallower (20–50 cm, e.g., [32]) whereas in the seasonal cycle temperature variations can go up to 10m depth [33]. This is mainly because much of the heat conducted through a soil profile is utilized to change the local temperature of the soil and there is a decrease in energy flux with depth. Thus, the phenomenon of amplitude damping, or a reduction in the magnitude of these temperature cycles with increasing depth is observed. As the annual average atmospheric temperatures continue to rise as well as the prevalence of drought conditions, it is likely that the seasonal temperature cycles are shifted to larger temperatures. While a higher soil shear strength is expected for drier conditions due to elevated levels of matric suction, the frequent wetting-drying cyclic changes will influence the soil macro and microstructure (e.g., development of a network of micro-cracks) that will in turn contribute to progressive deterioration of shear strength especially when compacted soil is subsequently exposed to wetting [34].

The atmospheric temperature together with relative humidity levels are the main drivers of the level of evaporation taking place although prevailing wind direction, vegetation type and cover, permeability and compaction conditions have been reported to also play a role [35]. The moisture variation in the ground also takes place up to a certain depth where the soil is likely to be subjected to wetting and drying cycles induced by from climatic changes. The rate of this change is typically dependent of the water retention behaviour of the soil, runoff and type of soil cover (bare, vegetation or impermeable) and the magnitude is controlled by climatic action, e.g., prevalence and patterns of rainfall or drought conditions. While the estimation of the depth of moisture change (H_s) is complex, a simple procedure based on local climate using Thornthwaite moisture index (TMI) distribution may be adopted. Table 4 shows the relationship between the depth of moisture change according to TMI values and type of climate classification for Australian Territories. The location of the site from which samples were collected can be classified as wet temperature with a TMI of 20 and thus depth of change of moisture would be 1.5–1.8 m. While there are other aspects related to soil behaviour such as water retention, permeability, compaction conditions and soil microstructure that strongly influence water flow in unsaturated materials, the TMI method provide a rough estimate of this depth.

Table 4. Depth of moisture change with Thornthwaite moisture index values (after [36]).

TMI	Classification	Depth of Moisture Change, H_s (m)
>40	Wet coastal	1.5
10 to 40	Wet temperate	1.5–1.8
–5 to 10	Temperate	1.8–2.3
–25 to –5	Dry Temperate	2.3–3.0
–40 to –25	Semi-arid	3.0–4.0
<–40	Arid	>4.0

This paper examines the comparative behaviour of various stabilisers used in industry, and shows their impacts on several variables, including Atterberg Limits, swelling and shear strength behaviour, microstructure and chemical composition. The results presented

directly showed the comparative effectiveness of these stabilisers for controlling volume change and shear behaviour of a natural expansive soil in roadworks or earthworks conditions. While all stabilisers were effective, HL was best to control one dimensional volume change whereas the specimens treated with PC showed the best performance in the post-inundation conditions. However, it should be noted that the greatest shear strength gains resulting from the stabiliser addition are limited to relatively small strains. This is reasonable as the soil is likely to experience levels of shear strain (1%) smaller or comparable to those reported at yield during service.

From an environmental footprint standpoint, each stabiliser can be compared by considering the embodied emissions of their production. As the emissions associated with transport, labour and machinery will vary depending on the location, source and means of application, these will be excluded from the calculation process. The embodied emissions of several of the materials used, as compiled by [37], can be seen in the Table 5 and corresponding embodied CO₂ calculated for the treatment levels adopted is shown in Table 6.

Table 5. Embodied emissions of Stabilisers.

Material	Emissions (kg CO ₂ /kg)
Hydrated Lime	0.74
Portland Cement	0.83
Ground granulated blast furnace slag	0.07

Table 6. Embodied emissions of stabilisers considered in the study for treatment levels adopted.

Material	Emissions (kg CO ₂)/Tonne of Treated Soil			
	1%	2%	3%	4%
Hydrated Lime (HL)	7.4	14.8	22.2	29.6
Portland cement (PC)	8.3	16.6	24.9	33.2
Ground Granulated Blast Furnace Slag (BFS)	0.7	1.4	2.1	2.8
BFS/HL (70/30) blend	2.71	5.42	8.13	10.84

It can be observed that the embodied emissions from the traditional stabilisers (Hydrated Lime and Portland cement), showed relatively high emissions, with between 0.7 and 0.83 kg of carbon dioxide emitted per kg of soil with each additional percent stabiliser added. In contrast, the use of GGBFS as a partial substitute for lime at the 70/30 ratio tested allows for a reduction in the embodied carbon of the materials by 63%. This is significant because the blend of SFS/HL has comparable performance in controlling volumetric changes derived from moisture ingress during inundation. This indicates that for this site the use of the SFS/HL is preferred to minimise carbon emissions. It should be noted that the carbon calculation presented in this paper refers to the production of the binders. In fact, there may be cases where the total embodied emissions (production, transport and application) of cement may be more competitive with the other binders owing to the proximity of a cement plant facility and a large volume of earthworks. For the road widening activities, i.e., location where the soil was collected, the use of SFS-HL would be more advantageous as the location is remote and the volume of earthworks is not extensive, however in larger infrastructure projects located near large industrial hubs the production footprint is balanced by transport, and cement and lime become more competitive in terms of CO₂ emissions. A detailed case by case study examining availability of binders and source location is recommended for each construction project to accurately quantify their carbon footprint. While in the study only conditions associated with extreme rainfall events were studied (full inundation), it is expected that long periods of drought cause cracking in

pavement underlain by expansive soil subgrade and hence exacerbate the effect of rainfall events, as water ingress is facilitated.

5. Conclusions

To evaluate the impact of climate change, in particular the simulation of a extreme rainfall event scenario, three different soil stabilisers commonly adopted in the road construction were considered. Both the improvement in terms of swelling and shear strength of a natural expansive soil were examined. The results of the one-dimensional tests series showed that while all stabilisers performed well in halting volumetric changes (swelling), hydrated lime at 4% showed the greatest performance, but Portland cement showed the greatest reduction in compression for the larger vertical stresses considered. In the terms of shear strength, all stabilisers were effective in improving peak strength, however the increase was marginal at ultimate state, likely due to the destructuring process of the soil structure during shearing. To simulate strain levels representative of service loads, the inundation at yield was considered. The secondary shearing phase results showed that Portland cement was the best performer followed by the blend of ground granulated blast furnace slag and hydrated lime (70:30). Despite its comparable performance in halting swelling and retaining higher shear strength upon inundation, the adoption of blends of ground granulated blast furnace slag and hydrated lime has been rather limited in road infrastructure. However, the results from this study clearly show that this blend is a viable option in comparison to more established carbon intensive stabilisers (Portland cement and hydrated lime) in the road construction. While the performance of only one blend incorporating blast furnace slag was studied, it shows encouraging potential for trial of other blends incorporating other types of slags, e.g., steel furnace slag.

Author Contributions: The contribution from the different authors can be summarised as follows. Conceptualization, A.H.; methodology, all authors; formal analysis, all authors; laboratory work and data curation, J.P. and T.K.; writing—original draft preparation, A.H.; writing—review and editing, all authors; supervision and project administration, A.H. All authors have read and agreed to the published version of the manuscript.

Funding: This research received no external funding.

Institutional Review Board Statement: Not applicable.

Informed Consent Statement: Not applicable.

Data Availability Statement: Not applicable.

Acknowledgments: The laboratory work reported herein was conducted at the soil testing facilities of the School of Civil, Mining and Environmental Engineering from the University of Wollongong. Authors appreciate the use the facilities and laboratory assistance provided by Richard Berndt. Assistance from Roads and Maritime Services in the expansive soil procurement is also gratefully appreciated.

Conflicts of Interest: The authors declare no conflict of interest.

References

1. Romero, E.; Gens, A.; Lloret, A. Water permeability, water retention and microstructure of unsaturated compacted Boom clay. *Eng. Geol.* **1999**, *54*, 117–127. [[CrossRef](#)]
2. Gens, A. Soil-environment interaction in geotechnical engineering. *Géotechnique* **2010**, *60*, 3–74. [[CrossRef](#)]
3. Alonso, E.E.; Pereira, J.M.; Vaunat, J.; Olivella, S. A microstructurally based effective stress for unsaturated soils. *Géotechnique* **2010**, *60*, 913–925. [[CrossRef](#)]
4. Heitor, A.; Indraratna, B.; Rujikiatkamjorn, C. The role of compaction energy on the small strain properties of a compacted silty sand subjected to drying-wetting cycles. *Géotechnique* **2015**, *65*, 717–727. [[CrossRef](#)]
5. Sun, D.; Sheng, D.; Xu, Y. Collapse behaviour of unsaturated compacted soil with different initial densities. *Can. Geotech. J.* **2007**, *44*, 673–686. [[CrossRef](#)]
6. Kodikara, J. New framework for volumetric constitutive behaviour of compacted unsaturated soils. *Can. Geotech. J.* **2012**, *49*, 1227–1243. [[CrossRef](#)]

7. Heitor, A.; Indraratna, B.; Rujikiatkamjorn, C. Laboratory study of small strain behaviour of a compacted silty sand. *Can. Geotech. J.* **2013**, *50*, 179–188. [[CrossRef](#)]
8. Zumrawi, M.M.E. Pavement Design for Roads for Expansive Clay Subgrade. *Univ. Khartoum Eng. J.* **2013**, *3*, 52–58.
9. CSIRO. *Climate Change in Australia*; Technical, Report; Whetton, P., Ed.; CSIRO: Canberra, Australia, 2015; ISBN 9781921232947.
10. Bureau of Meteorology, Long-Range Weather and Climate. Available online: <http://www.bom.gov.au/climate/> (accessed on 20 November 2020).
11. Buol, S.W.; Southard, R.J.; McDaniel, P.A.; Southard, R.J.; Graham, R.C.; McDaniel, P.A. *Soil Genesis and Classification*; John Wiley & Sons: Hoboken, NJ, USA, 2011.
12. Richards, B.G. Keynote Address'. In Proceedings of the Fifth International Conference on Expansive Soils, Adelaide, South Australia, 21–23 May 1984.
13. Erzin, Y.; Gunes, N. The unique relationship between swell percent and swell pressure of compacted clays. *Bull. Eng. Geol. Environ.* **2013**, *72*, 71–80. [[CrossRef](#)]
14. Erzin, Y.; Güneş, N. The prediction of swell percent and swell pressure by using neural networks. *Math. Comput. Appl.* **2011**, *16*, 425–436. [[CrossRef](#)]
15. Kassiff, G. Experimental Relationship between Swell Pressure and Suction. *Géotechnique* **2015**, *21*, 245–255. [[CrossRef](#)]
16. Sabtan, A.A. Geotechnical properties of expansive clay shale in Tabuk, Saudi Arabia. *J. Asian Earth Sci.* **2005**, *25*, 747–757. [[CrossRef](#)]
17. Tu, H.; Vanapalli, S.K. Prediction of the variation of swelling pressure and one-dimensional heave of expansive soils with respect to suction using the soil-water retention curve as a tool. *Can. Geotech. J.* **2016**, *53*, 1213–1234. [[CrossRef](#)]
18. Vanapalli, S.; Lu, L. A state-of-the art review of 1-D heave prediction methods for expansive soils. *Int. J. Geotech. Eng.* **2012**, *6*, 15–41. [[CrossRef](#)]
19. Jones, L.J.I. Chapter 3—Clay stabilization. In *Petroleum Engineer's Guide to Oil Field Chemicals and Fluids*, 2nd ed.; Fink, J., Ed.; Gulf Professional Publishing: Boston, MA, USA, 2015; pp. 121–145.
20. Yilmaz, I. Indirect estimation of the swelling percent and a new classification of soils depending on liquid limit and cation exchange capacity. *Eng. Geol.* **2006**, *85*, 295–301. [[CrossRef](#)]
21. Ferro, V.; Mirabile, S. Comparing particle size distribution analysis by sedimentation and laser diffraction method. *J. Agric. Eng.* **2009**, *2*, 35–43. [[CrossRef](#)]
22. Look, B.G. The weighted plasticity index in road design and construction. *Aust. Geomech.* **2016**, *51*, 21–35.
23. Nagaraj, H. Swelling behaviour of expansive soils. *Int. J. Geotech. Eng.* **2010**, *4*, 99–110. [[CrossRef](#)]
24. Austroads. *Pavement Design—A Guide to the Structural Design of Road Pavements*; Pavement Technology Series; Austroads Incorporated: Sydney, Australia, 2004.
25. Tasalloti, S.M.A.; Indraratna, B.; Rujikiatkamjorn, C.; Heitor, A.; Chiaro, G. A laboratory Study on the Shear Behaviour of Mixtures of Coal Wash and Steel Furnace Slag as Potential Structural Fill. *ASTM Geotech. Test. J.* **2015**, *38*, 361–372.
26. Cement Australia. *Safety Data Sheet*; Cement Australia Pty Ltd.: Darra, QLD, Australia, 2018.
27. Euroslag 2018, Properties: Slag. The European Association Representing Metallurgical Slag Producers and Processors. Available online: <http://www.euroslag.com/products/properties/> (accessed on 9 May 2018).
28. Al-Mukhtar, M.; Lasledj, A.; Alcover, J.-F. Behaviour and mineralogy changes in lime-treated expansive soil at 20 °C. *Appl. Clay Sci.* **2010**, *50*, 191–198. [[CrossRef](#)]
29. Take, W.A.; Bolton, M.D. Seasonal ratcheting and softening in clay slopes, leading to first-time failure. *Géotechnique* **2011**, *61*, 757–769. [[CrossRef](#)]
30. Ng, C.W.W.; Zhou, C. Cyclic behaviour of an unsaturated silt at various suctions and temperatures. *Géotechnique* **2014**, *64*, 709–720. [[CrossRef](#)]
31. Zhou, C.; Xu, J.; Ng, C.W.W. Effects of temperature and suction on secant shear modulus of unsaturated soil. *Géotech. Lett.* **2015**, *5*, 123–128. [[CrossRef](#)]
32. Wang, J.; Zheng, H. Experimental study on the effect of temperature and flux conditions on moisture distribution in vadose zone soil. *Water Sci. Technol.* **2017**, *75*, 881–889. [[CrossRef](#)]
33. Alam, M.R.; Zain, M.F.; Kaish, A.B.; Jamil, M. Underground Soil and Thermal Conductivity Materials Based Heat Reduction for Energy Efficient Building in Tropical Environment. *Indoor Built Environ.* **2015**, *24*, 185–200. [[CrossRef](#)]
34. Stirling, R.A.; Toll, D.G.; Glendinning, S.; Helm, P.R.; Yidiz, A.; Hughes, P.N.; Asquith, J.D. Modelling the deterioration of the near surface caused by drying induced cracking. *Géotechnique* **2020**. [[CrossRef](#)]
35. Glendinning, S.; Hughes, P.; Helm, P.; Chambers, J.; Mendes, J.; Gunn, D.; Wilkinson, P.; Uhlemann, S. Construction, management and maintenance of embankments used for road and rail infrastructure: Implications of weather induced pore water pressures. *Acta Geotech.* **2014**, *9*, 799–816. [[CrossRef](#)]
36. Fityus, S.; Buzzi, O. On the use of the Thornthwaite Moisture Index to infer depths of seasonal moisture change. *Aust. Geomech.* **2008**, *43*, 69–76.
37. Hammond, G.; Jones, C. *Inventory of Carbon & Energy: ICE*; Sustainable Energy Research Team, Department of Mechanical Engineering, University of Bath: Bath, UK, 2008; Volume 5.